Manipulation and decoherence of acceptor charge qubit in silicon

Y.P. Song and B. Golding
Department of Physics & Astronomy, Michigan State University, East Lansing, MI 48824-2230, USA

(Dated: November 20, 2010)

Dielectric constant and absorption measurement on boron doped silicon samples show that transitions between the acceptor energy levels can be induced by applied resonant ac electric field and stark tuning of level spacing by external DC electric field. The relatively longer decoherence time, $T_2^* = 2.6$ and $T_1 = 7.4\mu s$, was observed by electric echo measurement for low boron dopant concentration Si sample ($8\times10^{-12} cm^{-3}$). Scalable acceptor-based system is a promising candidate of charge qubit for quantum computing.

PACS number(s): 76.60.-k, 31.30.jn, 42.50.Pq

Intensive effect is currently underway to develop techniques and systems for quantum computing. In spite of the enormous progress in manipulating quantum systems and the demonstration of basic single- and two-qubit operations, no single implementation of a quantum computer has yet emerged as having an unmistakable advantage over other systems. Semiconductor-based quantum computers stand out as particularly attractive due to their promise of scalability and utilization of the vast knowledge and experience of the semiconductor fabrication industry. Spin-based systems are natural candidates for quantum computers, e.g., nuclear spins of ^{31}P donors,[1] or electron spins in semiconductor quantum dots,[2,3] as they take advantage of extremely long spin coherence times. However, their implementation is complicated by a number of issues got to be resolved. An alternative to the spin-based qubits is proposed by charge-based qubits formed by the low-lying states of the substitutional acceptor or donor in silicon.[4,5] Those systems do not depend on the single-spin readout and rely on a long-range electric-dipole interaction between the qubits for performing quantum logic operations. Therefore, the required spatial separation between the qubits is an order of magnitude larger than in the impurity-spin system,[1,6] which greatly simplifies fabrication.

Acceptors in silicon have been extensively studied and offer an attractive possibility for devising a quantum computer. The isolated shallow acceptor in silicon reflects the electronic structure of the $P_{3/2}$ valence band states at $k = 0$. As a concrete example, boron is a shallow acceptor in Si, substituting on the Si site, that lies 45 meV above the valence band maximum. The ground state has a 4-fold degeneracy that is split by external electric field or local strain. The resulting Kramers doublets form two working levels with $B = 0$ $m_J = \pm 1/2$ and $m_J = \pm 3/2$.[7, 8] The energy level spacing can therefore be controlled by external electric field, and the transitions between the energy levels can be induced by applied resonant ac electric field. Application of an external electric field by means of a surface gate allows the splitting to be precisely tuned in the microwave region. In this letter, we address the electrostatic tuning of energy level by stark effect for acceptors in silicon, which represents a centre for experimental realization of high precision control of acceptor in semiconductor. The electric echo spectroscopy is exploited to diagnose the qubit life time of acceptors in silicon. The absorption measurement and electric echo spectroscopy were performed on three samples: coplanar waveguide (CPW) resonator (sample 1), microstrip resonator (sample 2) on Si substrate with boron dopant concentration $2\times10^{15} cm^{-3}$ and low strain Si sample from Topsil with boron dopant concentration $8\times10^{12} cm^{-3}$ (sample 3).

Cavity quantum electrodynamics studies the properties of atoms coupled to discrete photon modes in cavities.[9] In CQED, an atomic two-level system is made to interact with the vacuum electric field E and the cavity presents a well defined electromagnetic environment to the qubit. Superconducting Nb coplanar resonator and microstrip resonator were made on (100) Si substrate by traditional UV photolithography techniques. Si substrate has 370um thickness with boron dopant concentration $2\times10^{15} cm^{-3}$. Superconductor niobium is chosen to make resonator due to its relatively large superconducting gap and small depth penetration. A 200nm thick Nb film is DC magnetron sputtered

for resonator pattern in Ar at 2×10^{-3} torr with a rate of 1 nm/s in an UHV system with a base pressure of 10^{-8} torr. The insert of Fig.1 illustrated a half-wave length coplanar resonator. The center conductor line of coplanar resonator has a 32.20 mm length and 0.45 mm width, separated 0.20 mm from the ground plate and capacitively coupled via its open end to a through line by a gap, resulting in the impedance $Z = 50$ ohm to match that of conventional microwave components. The microstrip line has a 27.56 mm length and 0.302 mm width separated 0.37 mm from the ground plate. To supply a DC bias to the resonator, a conductive pad connected to the center of the conductor line where the electric field of the microwave signal has a node, which minimizes any disturbance to the resonant microwave. The measured resonator with weak coupling to feeding line has high Q about 10^5. Considering relatively high cavity decay rate required for echo measurement, the resonators with appropriate Q were used for measurements. The resonator chip is mounted in a copper sample holder with two SMA connectors, which are connected to the through lines by two tiny bellows and connector tabs. Care was taken to design the sample holders to prevent the microwave leakage. The sample holder was loaded on the mix chamber of dilution refrigerator. Fig.1 shows a representative transmission power spectrum for coplanar device using HP network analyzer. Coplanar resonator has a resonance frequency at 1950.18 MHz with Q 1000 at 47mK. The total insertion loss is 18.4 dB at resonance frequency including the cable loss.

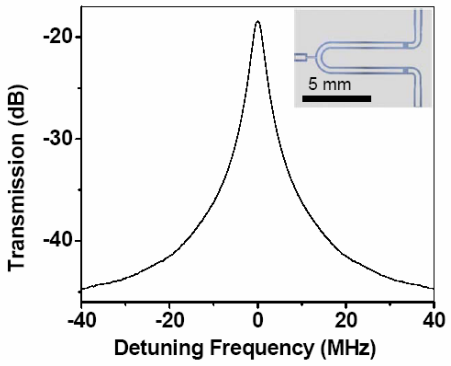

FIG.1: Measured transmission power spectrum of a λ/2 coplanar waveguide (CPW) resonator with resonance frequency 1950.18 MHz at 47mK. The insert illustrated the optical image of the measured resonator. A conductive pad connected to the center of the conductor line to supply a DC bias to the resonator.

The stark effect was investigated by applying DC voltage to center conductor line of coplanar resonator and investigating the absorption and dielectric constant change. Dielectric constant measurements involved monitoring the cavity resonance as a function of DC bias voltage by an amplifier lock-in technique. The resonant frequency f_0 of the half-wave length coplanar resonator is $f_0 = \frac{c}{2l\sqrt{\varepsilon_{eff}}}$, where c is the speed of light in vacuum, l is the resonator length and ε_{eff} the effective dielectric constant.[10, 11] Fig.2 shows the bias voltage dependence of the effective dielectric constant (red curve) and absorption (blue curve) for sample 1 at 36 mK. The resonator has a resonance frequency 1950.18 MHz at zero bias voltage. With increasing bias voltage, the resonant frequency shifts to higher frequency. Δf reaches 205.4 KHz at 20 V bias voltage, with the corresponding effective dielectric constant change $\Delta\varepsilon_{eff} / \varepsilon_{eff}$ -3.49×10^{-4}, where $\Delta f = f(V) - f(0)$ and $\Delta\varepsilon_{eff} = \varepsilon_{eff}(V) - \varepsilon_{eff}(0)$. Sweeping bias voltage from positive to negative, the bias voltage dependence is repeatable and almost symmetry to zero bias voltage, as shown in the top insert of Fig.2. The absorption was investigated by monitoring the total insertion loss change with sweeping bias voltage. The extracted bias voltage dependence of absorption is shown as the blue curve in Fig. 2. The curve is offset 18.4 dBm at zero bias voltage for clarity. The absorption rises with increasing bias voltage, which is consistent with dielectric constant measurement. Absorption of 0.035 dBm was found at 20 V compared to zero bias voltage. Recent experiments on superconducting micro-resonators observed temperature-dependent resonance frequency shifts and is very likely caused by two-level systems (TLSs) in dielectric material.[12, 13] The TLS states couple to the surrounding electric field through the electric dipole moments, which absorb and disperse energy when the energy level spacing matches hf_0, where f_0 is the resonance frequency.[14] TLS theory indicates that the electromagnetic absorption coefficient is proportional to $n\mu^2$, where n is the density of TLS states that couple to the electric field and μ represents the dipole moment.[15] Local strains due to dislocations, imperfections and lattice vibrations

are always present in silicon. Local strain will split the $P_{3/2}$ valence band into Kramers doublets by an amount $E_s = DS$, where D is the deformation potential and S is the internal strain.[16] Due to linear stark effect, the external electric field further lifts the energy level $|\vec{\varepsilon} * \vec{\mu}|$, where ε is external electric field and μ is the acceptor dipole moment. The bias voltage dependence of absorption reveals the charge state manipulation. The energy splitting contributes from both external electric field and local random strain depending on the relative directions of two fields. Due to the random characteristics of amplitude and direction for local strain, it is hard to map out the energy splitting caused by local strains directly, but the measurement results qualitatively reveal the local strain energy splitting distributes in a wide range ($\approx hf_0$), and the state density reduces with increasing splitting energy. The absorption is unsaturated when bias voltage goes up to 20V, which is in fact limited by the highest DC output of the voltage source we used. This indicates that the electric field is not high enough to shift the energy level out of microwave resonance.

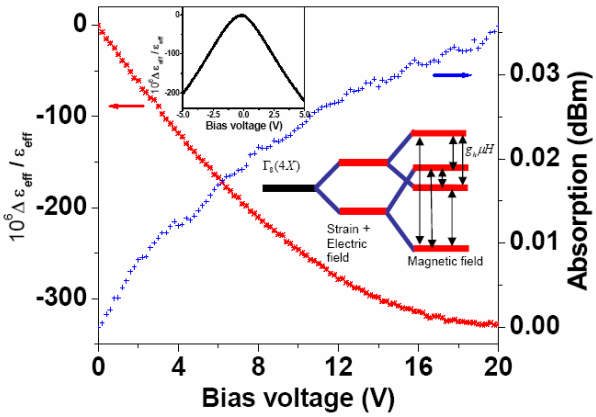

FIG.2: DC bias voltage dependence of the effective dielectric constant (red curve) and absorption (blue curve) for sample 1 (coplanar resonator device) at 36 mK. The absorption curve is offset 18.4 to 0 dBm at zero bias voltage for clarity. The top insert shows the effective dielectric constant change with sweeping bias voltage from 5V to -5V. The bias voltage dependence is almost symmetry to zero bias voltage. The right insert illustrates energy-level scheme for acceptor in silicon by external electric field and magnetic field in presence of random local strain. The multitude of possible transitions with different transition energies result in broadening of the transition line and prevent to observe the absorption enhancement.

The Kramers doublet can be further split in a magnetic field H and each band is split by the Zeeman energy $E_Z = g_h \mu H$, where μ is the Bohr magneton and g_h the hole g value. The dielectric constant measurement was performed on a low strain boron doped Si sample (sample 3) by monitoring the cavity resonance frequency shift as a function of the magnetic field. The sample has cylinder shape with 10mm diameter and 4mm thickness. The sample was placed in the uniform electric field region of a re-entrant cavity with resonance frequency 1.77 GHz. The cavity was cooled down to 45 mK by attaching it to the mixing chamber of dilution refrigerator. The magnetic field is parallel to Si [100] direction. It is expected that absorption enhancement would occur when the Zeeman splitting energy matches hf_0 . Sweeping magnetic field from 0 to 6000 Oe, the dielectric constant change (resonance frequency) shows a wide valley (peak) in the magnetic field range between 1518 and 2220 Oe reflecting an absorption enhancement, as shown in Fig. 3 (black curve). Sweeping magnetic field back from 6000 to 0 Oe shows the similar field dependence (red curve). In presence of local strain and magnetic filed, a variety of situations of energy splitting can arise, depending on the relative directions of the two fields, their orientations with respect of the silicon crystal axes, and the relative strength of the two fields. In the situation of strain energy E_s less than Zeeman energy E_z , the energy bands may be characterized by the quantum number $m_j = 3/2$, $1/2$, $-1/2$ and $-3/2$, and the energy-level scheme can be shown in the insert of Figure 3. The absorption enhancement is most likely caused by the low energy transition between $\pm 1/2$ levels. The extracted $g_{1/2}$ is 0.83 corresponding to the "dip" position at 1518 Oe, which is close to the reported g_h value for boron acceptor in Si.[8, 17]. It is noted that the absorption enhancement occurs in a wide range. It may be due to the random direction of local strain with respect to the magnetic field orientation, resulting in the different effective g values. The spin-state mixing may also contribute to wide-range absorption enhancement. Coplanar resonator device (sample 1) shows a different magnetic field dependence. By sweeping magnetic field from 0 to 6000 Oe with direction in (100) plane, no obvious absorption enhancement was found at bias voltage 0 and 19 V.

Compared with the low strain Si:B sample, the energy splitting caused by local strain is larger in sample 1. If E_s is in an order of $g_h \mu H$, the Zeeman splitting bands are not characterized by a given m_J quantum number, and all the six spin transitions are allowed with different g values.[16] The multitude of possible transitions with different transition energies therefore results in broadening of the transition line, which makes it difficult to observe the absorption enhancement.

Long decoherence time is highly desired for quantum computer operation, which determine how many quantum operations can be carried out in the duration of relaxation time. It is critical to probe the homogeneity of the acceptor environment and measure the dephasing time T_2^* and longitude relaxed time T_1. Decoherence time has been measured by electron spin resonance (ESR) experiments for the qubit based on donors in silicon.[18] However, few studies have been conducted on the dynamics of charge qubit based on acceptors in semiconductor. The electric echo measurement was performed on sample 1, however, no echo signal was detected. Considering the limit penetration depth of electric field for CPW geometry, it is not surprising that no echo signal was found because there are only less than 10^{10} states contributing to state manipulation. The echo measurements were then conducted on sample 2, which has relatively larger acceptor states 6.2×10^{12}. Microwave pulse sequence was applied to cavity with resonance frequency 2.01 GHz. Care was taken to keep the duty cycle low enough so that bulk heating of the sample did not occur. The echo signal was amplified and mixed with LO signal, and then readout by a Lecroy oscilloscope. Dephasing time T_2^* was measured by two electric pulses separated by a time τ_{12}, which produce an echo of amplitude $E = E_0^j \sin\theta_j \sin^2(\theta_j/2)$ after an additional time τ_{12}, where $\theta_j = (\mu_j/\hbar)F\tau$, μ_j is the electric dipole moment of acceptor j, F is pulse amplitude and τ is pulse duration.[19, 20] Echo amplitude decays as a function of τ_{12} with $\exp(-2\tau_{12}/T_2^*)$. Fig.4a (black dots) shows the relative echo amplitude versus τ_{12} for sample 2. Fitting an exponential to the time dependence of echo amplitude yields a dephasing time $T_2^* = 1.58\mu s$ at 45 mK. A three-pulse excitation sequence was used to measure longitudinal relaxation time T_1.[20] This stimulated-echo sequence consists of two $\pi/2$ pulses separated by a time τ_{12}, a third $\pi/2$ pulse at time $\tau_{13}+\tau_{12}$, and an echo after an additional time τ_{12}. The exponential decay of echo amplitude as a function of $\tau_{13}+2\tau_{12}$ provides a characteristic relaxation time T_1 ($\tau_{13} >> T_2^* > \tau_{12}$). Three pulse sequence echo shows an exponential decay in Fig.4B (black dot) with longitudinal relaxation time $T_1 = 4.0\mu s$ at 45 mK. The echoes seen here were generated by about 6.2×10^{12} acceptor states and the average acceptor-acceptor distance is around 80nm. Interactions between acceptors lead to decoherence and limit the coherence lifetime. The longer acceptor distance leads to weaker interaction, resulting in longer coherence lifetime. Compared to sample 2, low strain Topsil Si:B sample (sample 3) has same order of acceptor states 2.5×10^{12} but much longer inter-acceptor

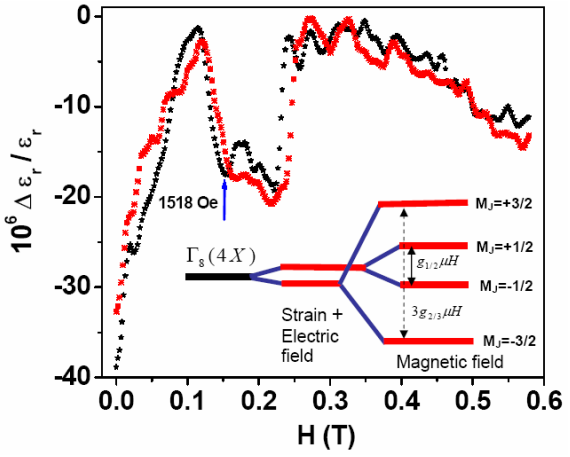

FIG.3: The measured effective dielectric constant change with sweeping magnetic field between 0 and 6000 Oe for low strain Si:B sample at 45mK. The magnetic field dependence indicates an absorption enhancement in the magnetic field range between 1518 and 2220 Oe. Upward field sweep (black curve) and downward field sweep (red curve) have similar field dependence. The insert shows acceptor energy-level scheme by external electric field and magnetic field for the sample. The energy bands are characterized by m_J quantum numbers and the allowed spin transitions are $\Delta m_J = \pm 1$.

spacing of order 500nm. Sample 3 was used for two and three-pulse sequence echo measurements to probe the relaxation time for acceptor states with weaker interaction. The red dots in Fig.4a and b show T_2^* and T_1 measurement results for sample 3 at 45 mK, respectively. The relative longer characteristic relaxation time, $T_2^* = 2.6$ and $T_1 = 7.4\mu s$, were found, which is consistent with expectations. The echo decay for sample 3 deviates from exponential law when $\tau_{12} > 4\mu s$ for T_2^* and $\tau_{13} > 10\mu s$ for T_1, which is found for sample 2 with $\tau_{12} > 3\mu s$ for T_2^* as well. This deviation may come from other tunneling centers rather than boron acceptors with different dipole moment or from the fact that the interaction between these tunneling centers may not be dipolar.[20]

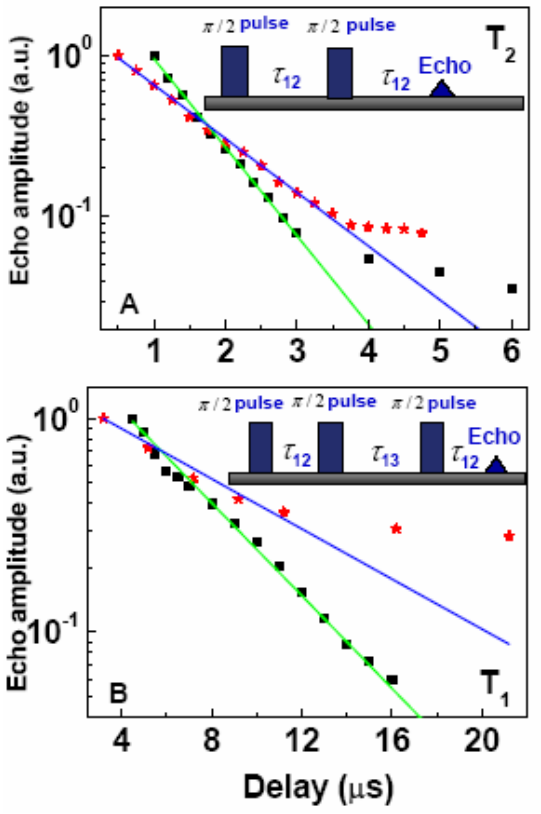

FIG.4: (A) Two-pulse echo decays for sample 2 and sample 3 at 45 mK. The black dots and red dots show the relative echo amplitude versus τ_{12} for sample 2 and sample 3, respectively. Fitting an exponential to the time dependence of echo amplitude yields the dephasing time $T_2^* = 1.58\mu s$ and $2.6\mu s$ for sample 2 (green solid line) and sample 3 (blue solid line), respectively. (B) Longitudinal relaxation time T_1 measurement by three-pulse excitation sequence for sample 2 and sample 3 at 45 mK. The black dots and red dots show the relative echo amplitude versus $\tau_{13} + 2\tau_{12}$ for sample 2 and sample 3, respectively. Exponential Fitting yields a relaxation time $T_1 = 4.0\mu s$ and $7.4\mu s$ for sample 2 (green solid line) and sample 3 (blue solid line), respectively.

Dielectric constant and absorption measurement on boron doped silicon samples indicate that transitions between the energy levels of acceptor state can be induced by applied resonant ac electric field and stark tuning of level spacing by external electric field. By sweeping magnetic field, an absorption enhancement was observed for low strain Si:B sample when Zeeman splitting energy matching cavity photon energy, while large energy splitting distributions due to random local strain prevent absorption enhancement in normal boron doped silicon sample. The electric echo spectroscopy is performed to detect acceptor decoherence time. The results show the interactions between acceptors reduce the coherence lifetime, and relatively longer decoherence time, $T_2^* = 2.6$ and $T_1 = 7.4\mu s$, was found for low boron dopant concentration sample ($8\times10^{12}\,cm^{-3}$). The acceptor in low strain silicon is a promising candidate of charge qubit for quantum computing. The acceptor-based system is scalable, since the acceptors can be arranged on a planar array on an order of 100nm grid. The two states of a qubit are the lowest orbital states of the acceptor, a result of splitting of the ground state by electric field. Each acceptor is addressed by an individual gate that imposes a static electric field, and tunes the level spacing via the Stark effect. The single-qubit operations can be therefore done by applying a radiation pulse and simultaneously tuning a targeted qubit into resonance. Two-qubit operations are enabled by long-range dipolar interaction between the acceptors, which in turn allows the qubit-qubit distance to be more than 100nm, while keeping a high clock rate near 10^8 Hz.[4] The readout of the final state of the computer can be based on quantum nondemolition optical measurement of resonant Rayleigh scattering by an exciton bound to the acceptor.[21]

Acknowledgment: This research is supported by NSF-ITER grant. The authors thank Prof. M.I. Dykman for useful discussions and Baokang Bi for access to clean room facilities.

* Electronic address: y34song@uwaterloo.ca

[1] R. G. Clark, R. Brenner, T. M. Buehler, V. Chan, N. J. Curson, A. S. Dzurak, and E. Gauja, Phil. Trans. R. Soc. Lond. A **361**, 1451 (2003).

[2] R. Hanson, L. P. Kouwenhoven, J. R. Petta, S. Tarucha, and L. M. K. Vandersypen, Rev. Mod. Phys **79**, 1217 (2007).

[3] K. Ono, D. G. Austing, Y. Tokura, and S. Tarucha, Science **297**, 1313 (2002).

[4]B. Golding and M.I. Dykman, arxiv.org/pdf/cond-mat/0309147.

[5] V. N. Smelyanskiy, A. G. Petukhov, and V. V. Osipov1, Phys. Rev. B **72**, 081304 (2005).

[6] B. E. Kane, Nature **393**, 133 (1998).

[7] P.E. Vanier, and A. Honig, J. Phys. Chem. Solids **45**, 495 (1984).

[8] F. Merlet, B. Pajot, P. Arcas, and A. M. Jeanlouis, Phys. Rev. B **12**, 3297 (1975).

[9] B. Alexandre, H. Ren-Shou, W. Andreas, S. M. Girvin, and R. J. Schoelkopf, Phys. Rev. A **69**, 062320 (2004).

[10] M. Shigenobu, T. Masafumi, S. Tomotaka, H. Shigeki, N. Hiroaki, F. Akira, N. Masaya, T. Hitoshi and K. Tomoji, Supercond. Sci. Technol. **15**, 635 (2002).

[11] M. A. Hussein, S.J. Ahmad, and M.R. Sedki, IEEE Trans. Inst. Meas. **55**, 2216 (2006).

[12] G. Jiansong Gao, D. Miguel, V. Anastasios, K. Shwetank, Z. Jonas, S. Bernard, A.M. Benjamin, K.D. Peter, and G.L. Henry, Appl. Phys. Lett. **92**, 152505 (2008).

[13] K. Shwetank, G. Jiansong, Z. Jonas, A.M. Benjamin, G.L. Henry, and K.D. Peter, Appl. Phys. Lett. **92**, 123503 (2008).

[14] D.O. Aaron, M. Ansmann, R.C. Bialczak, M. Hofheinz, N. Katz, and L. Erik, Appl. Phys. Lett. **92**, 112903 (2008).

[15] M. VonSchickfus, and S. Hunklinger, Phys. Lett. A **64**, 144 (1977).

[16] G. Feher, J.C. Hensel, and E.A. Gere, Phys. Rev. Lett. **5**, 309 (1960).

[17] J.M. Cherlow, R.L. Aggarwal, and B. Lax, Phys. Rev. B **7**, 4547 (1973).

[18] T. Schenkel, J.A. Liddle, A. Persaud, A.M. Tyryshkin, S.A. Lyon, R. Sousa, K.B. Whaley, J. Bokor, J. Shangkuan, and I. Chakarov, Appl. Phys. Lett. **88**, 112101 (2006).

[19] G. Brage, M.V. Schickfus, S. Hunklinger, and K. Dransfeld, Phys. Rev. Lett. **43**, 1817 (1979).

[20] M.C. Foote, and G. Brage, Phys. Rev. B **43**, 9206 (1991).

[21] S.W. Koch, M. Kira, G. Khitrova, and H.M. Gibbs, Nature Mater. **5**, 523 (2006).